Analysis and Optimization of Quantitative Magnetization Transfer Imaging Considering the Effect of Non-Exchanging Component

Pouria Mossahebi[1], Andrew L Alexander[2,3], Aaron S Field[1,4], and Alexey A Samsonov[4]

[1]*Biomedical Engineering, University of Wisconsin, Madison, WI, United States,* [2]*Medical Physics, University of Wisconsin, Madison, WI, United States,* [3]*Waisman Lab for Brain Imaging and Behavior, University of Wisconsin, Madison, WI, United States,* [4]*Radiology, University of Wisconsin, Madison, WI, United States*

INTRODUCTION: Gray matter demyelination has recently been recognized as an important pathological substrate of multiple sclerosis disease [1,2]. Magnetization transfer imaging (MTI) including both semi-quantitative (MT ratio) and quantitative (qMTI) approaches [3-6] has demonstrated high sensitivity to myelination in white matter [7,8]. Its applications to cortical gray matter characterization, however, we need to take into account additional factors related to anatomical organization of cortical GM such as partial volume effect (PVE) with CSF, the significant confounder in many qMRI techniques [9,10]. Recently, we proposed a theoretical model [11] that allows isolating a voxel compartment that is under slow or no-exchange (NE) conditions with the MT subsystem associated with the macromolecular-rich tissue. PVE with CSF may be described by such NE-compartment and hence may be potentially accounted by the qMT modeling to provide unbiased estimation of myelin-sensitive measures such as macromolecular pool fraction [12]. In this work, we analyze the effect of NE component on qMT and MTR parameters and provide results of numerical, phantom and in-vivo validation of the approach as a way to minimize underestimation of qMT measures due to PVE. Additionally, we developed a fast-optimized protocol for in-vivo application of NE-mCRI.

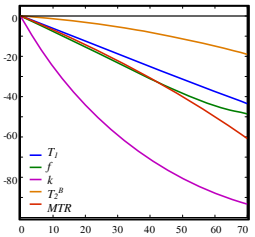

Fig 1. Percent Error in MT measures vs. NE fraction(%)

METHODS: NE-mCRI is built on modified cross-relaxation imaging (mCRI) method [4,13], which estimates the standard two-pool MT model parameters such as bound pool fraction f, cross-relaxation rate k, and T_2 of the bound pool T_2^B and parameters of the third pool associated with NE compartment. The estimation is performed by fitting the corresponding model to several SPGR datasets and MT-weighted SPGR datasets sensitive to both MT and NE subsystems of the model. *Simulation:* To estimate errors in the qMT parameters and MTR caused by PVE, synthetic VFA and MT SPGR signal intensities were generated using the three-pool model for GM (R_1 =0.71s^{-1}; f =8.8%; k=1.57s^{-1}; T_2^B=10.21μs) with the pulse sequence parameters of the in vivo study. The signals were then fit by the two-pool mCRI model. Additional numerical simulations were used to compare the accuracy in fitting 2-pool (mCRI) and 3-pool (NE-mCRI) models over the range of experimental conditions. Theoretical data were generated using the 3-pool model [11] for the range of brain bound pool fraction f (%)=(2,4,6,8,10,12,14,16,18, and 20) in the presence of different amount of NE_f(%)=(0,5, 10,15,20,25,30,35,40,45, and 50). This provided a 10×11 bound pool fraction vs. non-exchanging fraction grid. For each simulation, 10,000 signals were generated from theoretical data with Gaussian-distributed additive noise. The parameters of each model were estimated by fitting the synthetic data to both 2-pool and 3-pool models.

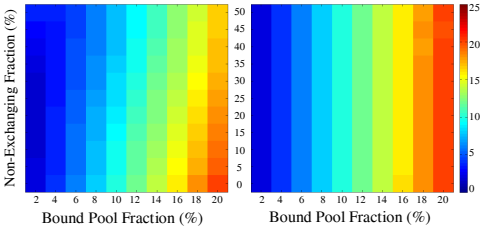

Fig 2. 2-pool (left) and 3-pool (right) simulation results.

Phantom and Healthy Volunteer Experiments: All data were acquired on a 3.0T GE MR750 scanner. Flip angle (B_1) and field (B_0) maps were measured by AFI [14] and IDEAL [15]. 25% cylindrical shape gelatin phantom (covered by plastic wrap to prevent diffusion exchange) was placed in the water bath. The imaging plane was tilted in respect to the phantom to introduce PV from surrounding water varying along the phantom axis. SPGR and MT-SPGR data were acquired with the same TR/TE/image matrix (3D SPGR data: α=[3,7,19,40]˚; MT VFA SPGR data with all combinations of (α=19˚,Δ=2.5,5,9,13kHz, α_{MT}=[800,1300]˚) and (α=[3,7,40]˚,Δ=2.5,13kHz,α_{MT}=[800,1300]˚). The data at α=7˚, Δ=2.5kHz, α_{MT}=1300˚ and corresponding SPGR data was used to calculate MTR. The optimized human protocol (Monte-Carlo simulations) includes three VFA SPGR (α=[4,14,26]˚, T_R/T_E =23/2.0ms) and five MT VFA SPGR (Δ(kHz)/α_{MT}/α = 2/1170˚/4˚, 2/1170˚/14˚,2/1170˚/26˚,2/600˚/14˚,8/1170˚/14˚) with T_R/T_E= 40/2.0ms. All Z-spectroscopic and VFA data were acquired with FOV=220×220×176mm and matrix=150×150×44. 4mm slice thickness was prescribed to introduce more PVE and better appreciate the correction by NE-mCRI method.

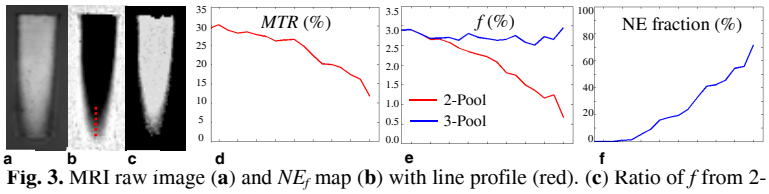

Fig. 3. MRI raw image (**a**) and NE_f map (**b**) with line profile (red). (**c**) Ratio of f from 2-pool to 3-pool **d,e,f:** line profile results.

RESULTS: *Simulations:* PVE with NE component progressively decreases apparent estimates of MTR and all parameters of 2-pool MT model with k and T_2^B being most and least affected, respectively (Fig.1). Fig. 2 shows the estimated bound pool fraction across the range of f and NE_f values for both 2-pool and 3-pool models. The standard 2-pool method increasingly underestimates the f as the NE_f increases, while the 3-pool method correctly estimates the f for the range of NE_f, which can be appreciated by the uniform bound pool fraction estimated for each f for the range of NE_f (across each column). *Phantom Studies:* The NE water fraction estimated by NE-mCRI (3-pool) increases along the tilted phantom. These changes are accompanied by a decrease in MTR and f estimated by standard two-pool model mCRI. NE-mCRI estimate of f shows much less variability along the phantom reflecting uniform composition of MT phantom rather than macroscopic partial volume with surrounding water. *In Vivo:* Fig. 4 illustrates effect of CSF PVE modeling on qMT parameters using 2-pool model and its correction by the 3-pool model. The removal of partial volume effect by CSF markedly increases the apparent size of GM structures on f map in the areas with PVE from CSF (bordering the ventricles, red arrows in Fig. 4). Difference maps between two models parameters better show the correction using 3-pool model on PV region, which are consistent with the simulation results (Fig.1) showing highest error in k and lowest error in T_2^B. Model preference is quantified by both residual maps comparison (showing higher residuals with 2-pool model especially in PVE with CSF) and Bayesian information criterion (BIC) map showing 3-pool is preferred for the majority of brain voxels.

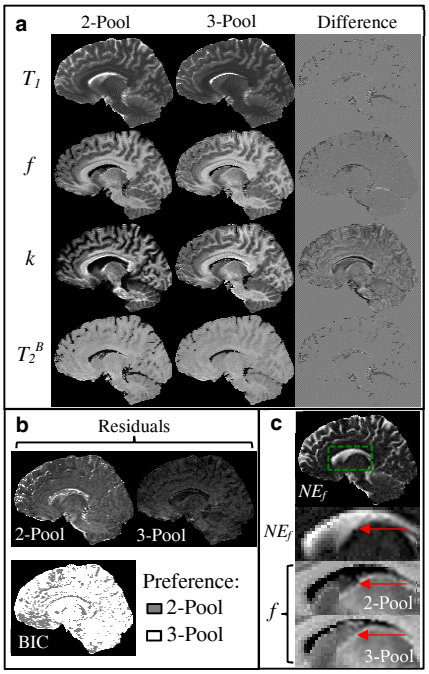

Fig. 4. (**a**) In-vivo qMT parameter results generated using different models. (**b**) Residual and BIC maps. (**c**) Zoom view of the boxed area.

DISCUSSION: This work establishes feasibility of estimating the third pool (NE component) in addition to the standard two-pool qMT parameters from a set of MT-weighted SPGR data. Our results indicate that such estimation can be performed quite robustly for the range of f values for both normal and demyelinated tissues (Fig. 2). As GM-CSF PVE may be significant at typical resolutions of qMRI techniques [9,10], CSF may be a serious confounder for MT-based characterization of GM myelination using either MTR or f potentially affecting voxel-wise and histogram analyses (Fig. 1). Our results demonstrate that explicit modeling of PVE using our NE-mCRI approach efficiently corrects CSF PVE biases in qMTI (Figs. 3,4). It was noted before that increasing CSF PVE with developing brain atrophy in the course of MS disease reduces apparent values of MT contrast histogram [16]. Such effect inevitably reduces specificity of MTI to myelination, making it sensitive to both demyelination and atrophy. Removal of PVE from qMT measurements may improve characterization of myelin status in cortical GM especially in subpial regions.

REFERENCES: [1] Kutzelnigg A, Brain 2005. [2] Kidd T, Brain 1999. [3] Sled JG, MRM 2001. [4] Yarnykh VL, MRM 2002. [5] Tozer D, MRM 2003. [6] Yarnykh VL, Neuroimage 2004. [7] Samsonov A, Neuroimage 2012. [8] Underhill HR, NeuroImage 2011. [9] Deoni SC, MRM 2012. [10] Yang AW, JMRI 2013. [11] Mossahebi P, ISMRM 2013. [12] Yarnykh VL, MRM 2012 [13] Mossahebi P, MRM 2013. [14] Yarnykh VL, MRM 2007. [15] Reeder SB, MRM 2005. [16] Kalkers NF, J Neurol Sci 2001.

ACKNOWLEDGEMENTS: This work was supported by NIH (R01NS065034).